

Sussex Research

Amacrine cells differentially balance zebrafish color circuits in the central and peripheral retina

Xinwei Wang, Paul Roberts, Takeshi Yoshimatsu, Leon Lagnado, Thomas Baden

Publication date

28-02-2023

Licence

This work is made available under the [CC BY 4.0](#) licence and should only be used in accordance with that licence. For more information on the specific terms, consult the repository record for this item.

Document Version

Published version

Citation for this work (American Psychological Association 7th edition)

Wang, X., Roberts, P., Yoshimatsu, T., Lagnado, L., & Baden, T. (2023). *Amacrine cells differentially balance zebrafish color circuits in the central and peripheral retina* (Version 1). University of Sussex.
<https://hdl.handle.net/10779/uos.23309150.v1>

Published in

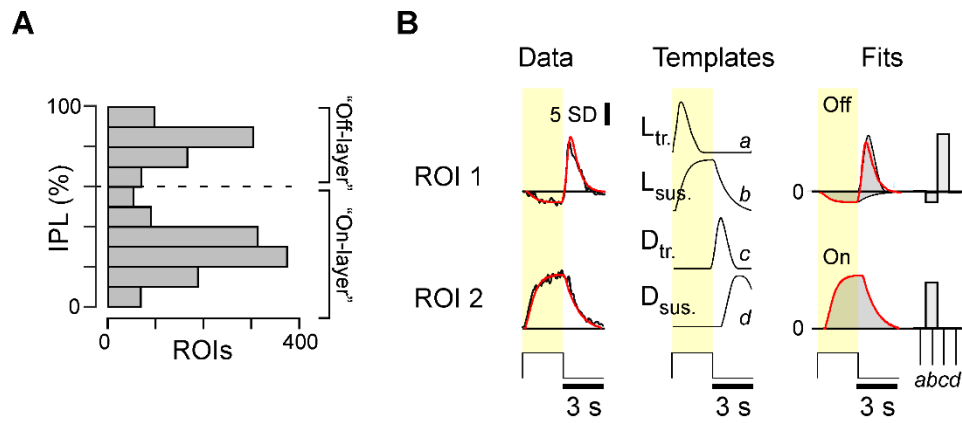
Cell Reports

Link to external publisher version

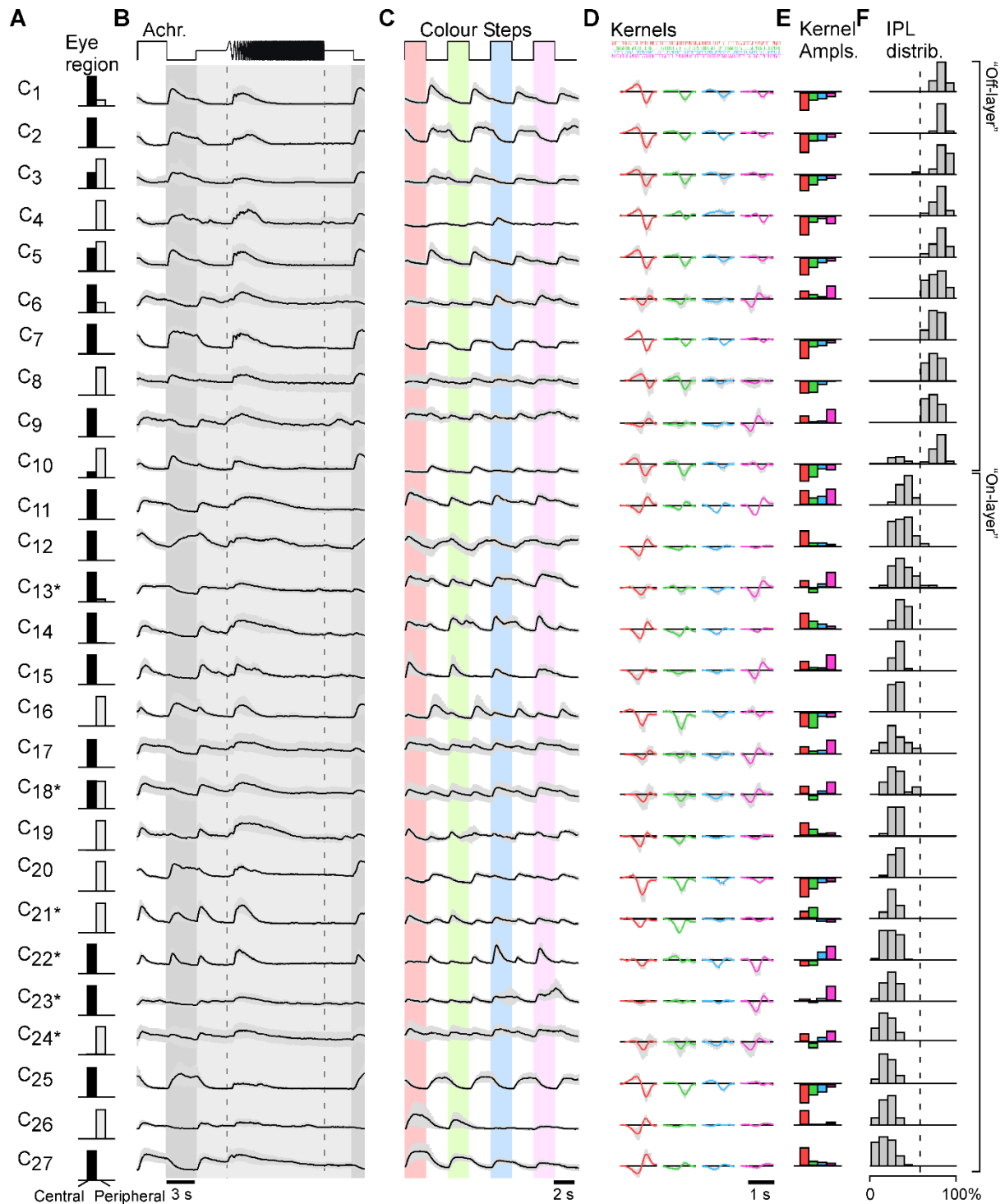
<https://doi.org/10.1016/j.celrep.2023.112055>

Copyright and reuse:

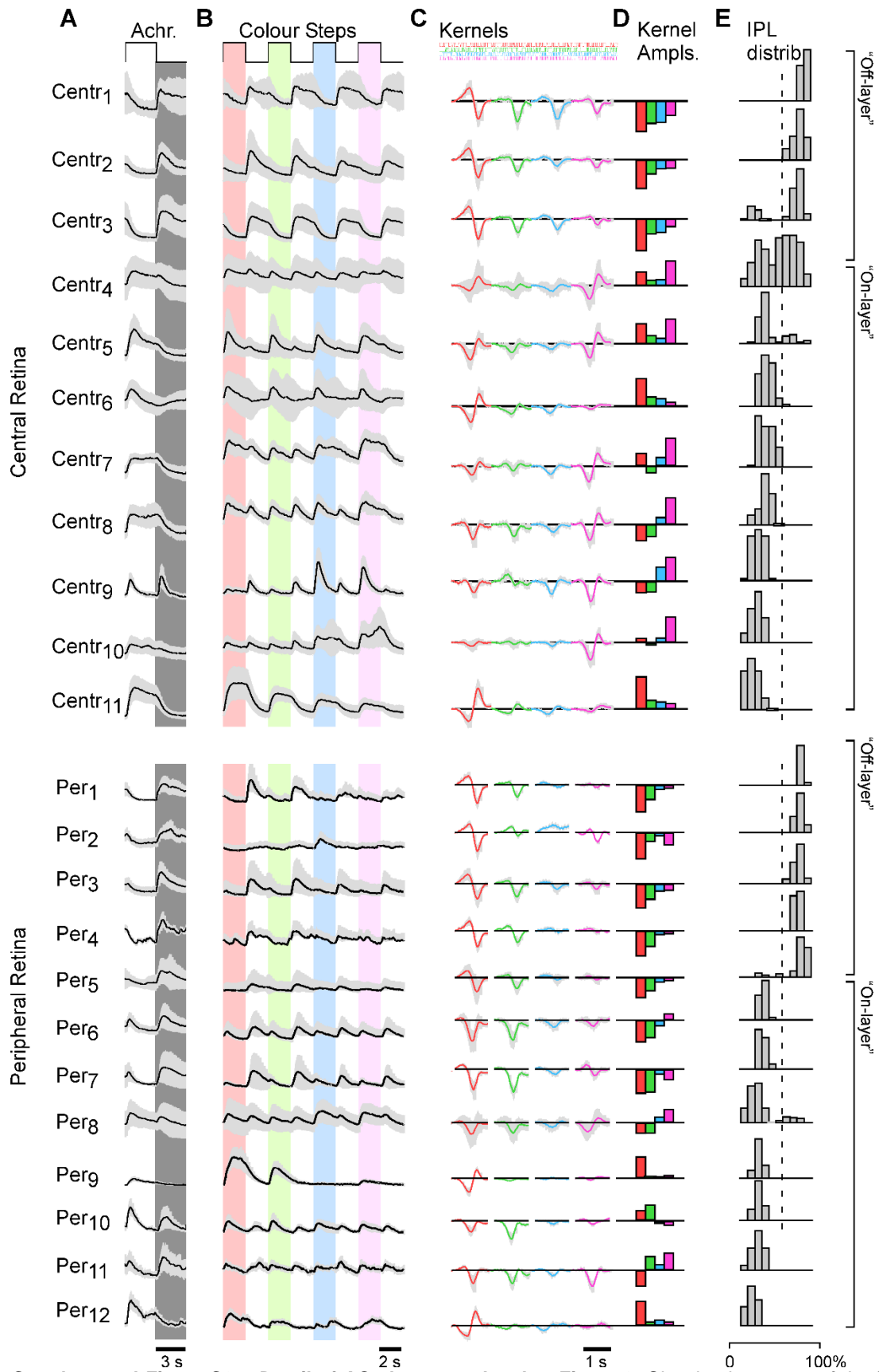
This work was downloaded from Sussex Research Open (SRO). This document is made available in line with publisher policy and may differ from the published version. Please cite the published version where possible. Copyright and all moral rights to the version of the paper presented here belong to the individual author(s) and/or other copyright owners unless otherwise stated. For more information on this work, SRO or to report an issue, you can contact the repository administrators at sro@sussex.ac.uk. Discover more of the University's research at <https://sussex.figshare.com/>



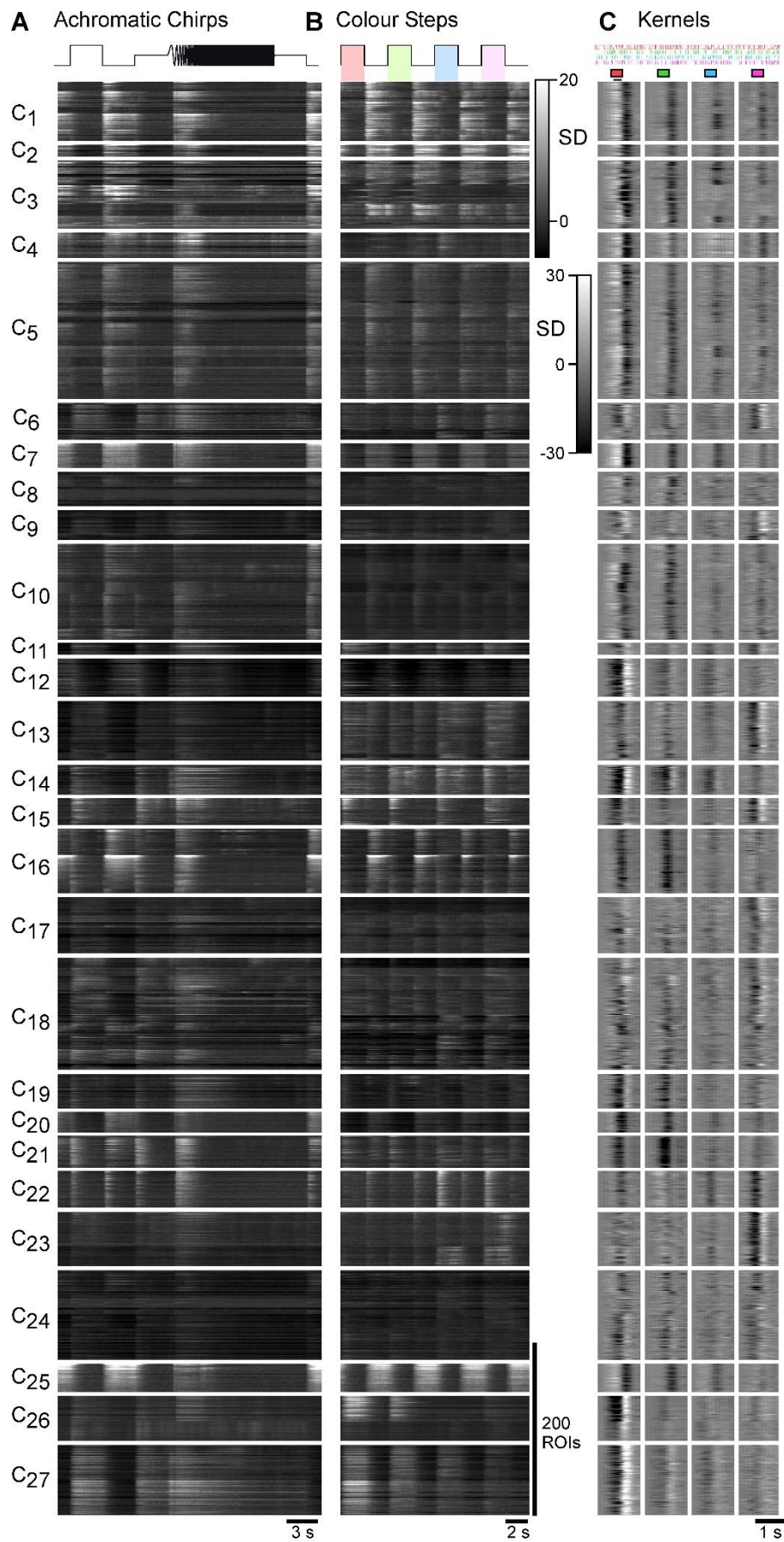
Supplemental Figure S1 – IPL distribution of the AC-ROIs and template-fitting method, related to Figure 1. **A**, distribution of all AC-ROIs across the IPL. **B**, Kinetic template-fitting approach (Methods) illustrated using the white-step responses of example ROIs 1 and 2 (Figure 1D). Left: Response means (black) shown with the fit superimposed (red). Middle: Four kinetic templates are used for fitting: Light-transient, Light-sustained, Dark-transient, and Dark-sustained. Right: scaled kinetic components used to fit the two example ROIs (grey) with their sum superimposed (red), and corresponding component weights (bars).



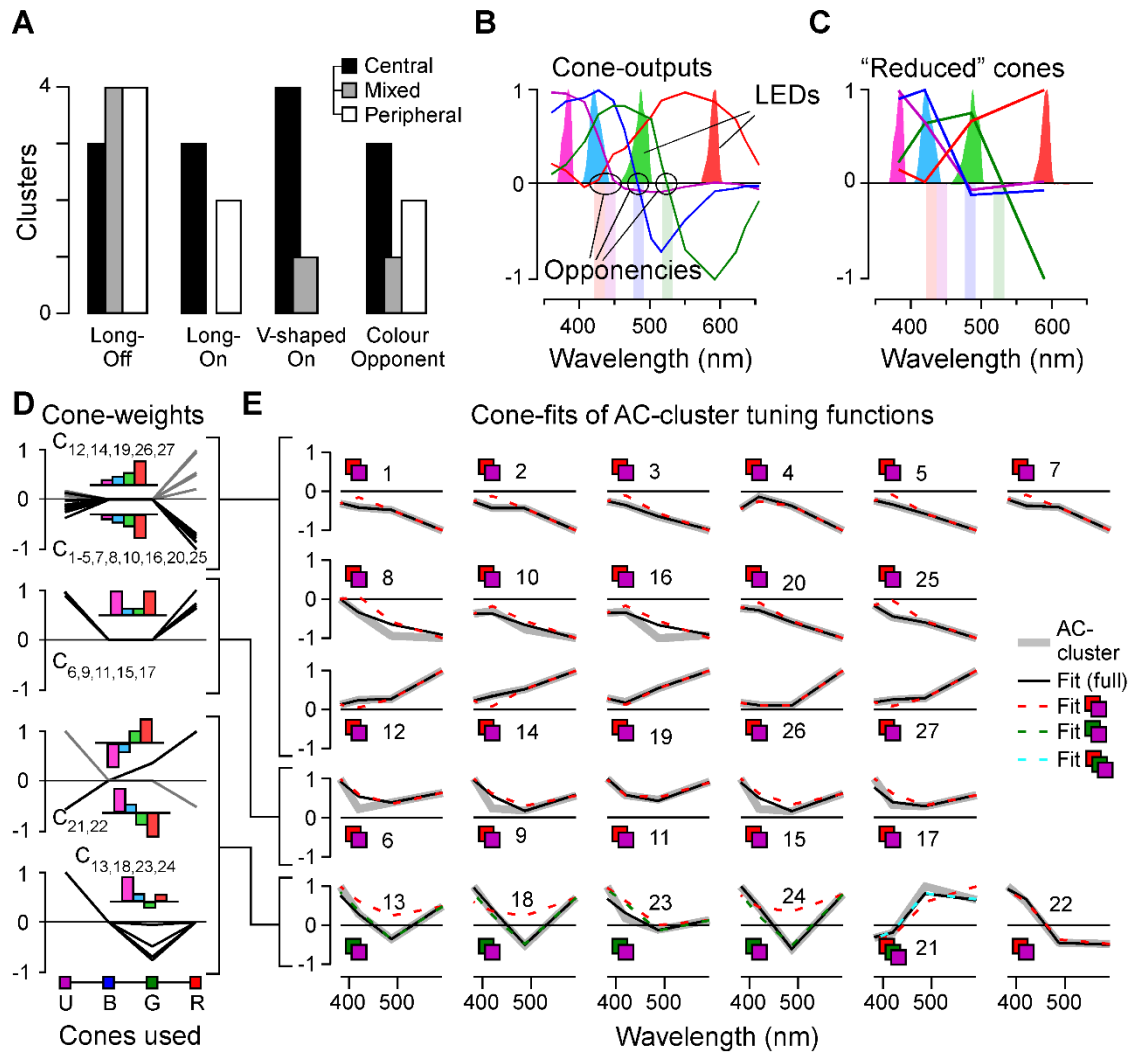
Supplemental Figure S2 – Full cluster overview of ACs, related to Figure 2. Shown are the eye region of the included ROIs (A, Central / Peripheral), as well as the mean \pm SD of chirps (B), color-steps (C), Kernels (D), mean kernel amplitudes (E) and IPL distribution of included ROIs normalised to the population of all recorded ROIs (cf. Supplemental Figure S1A).



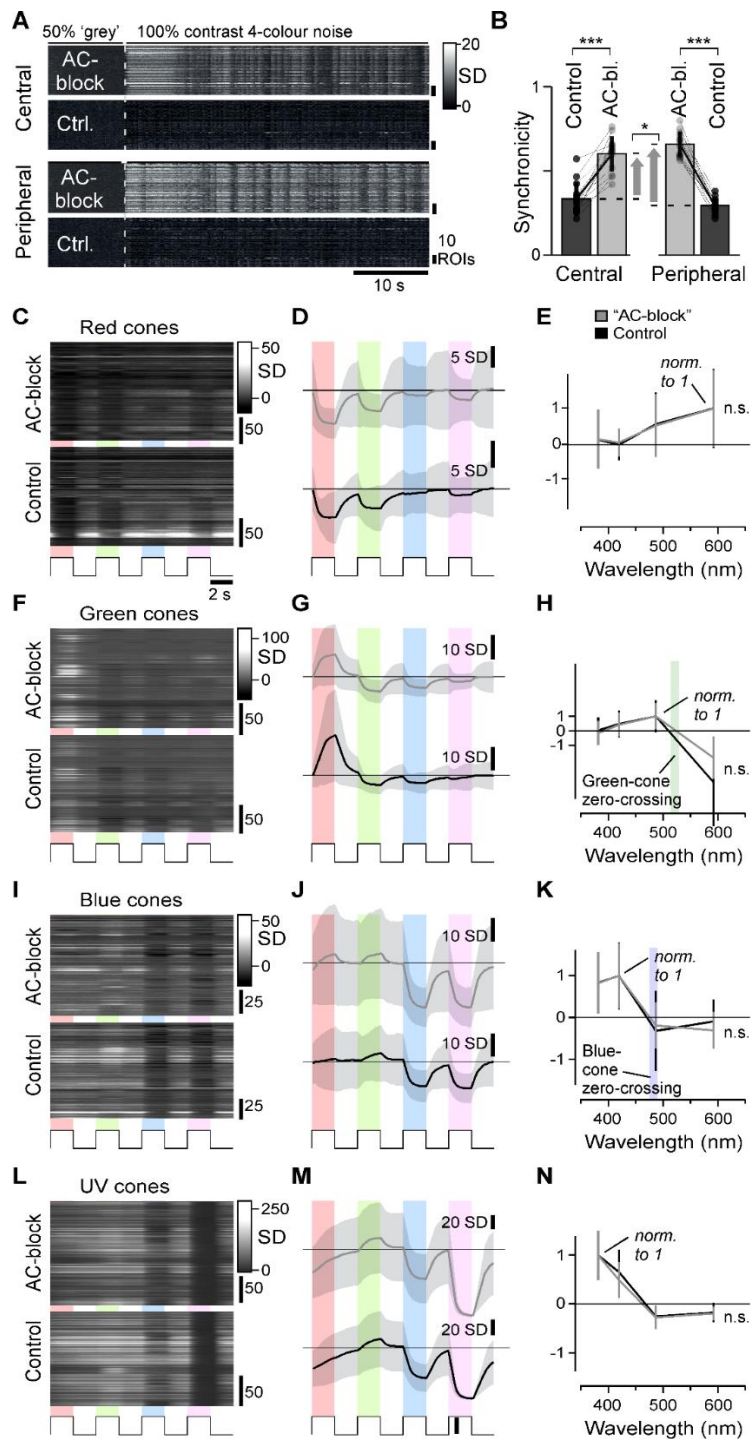
Supplemental Figure S3 – Detail of AC clusters, related to Figure 2. Showing heatmaps of the full dataset leading to the cluster means shown in Supplemental Figure S2. Shown are the chirps (A), colour-steps (B), and kernels (C).



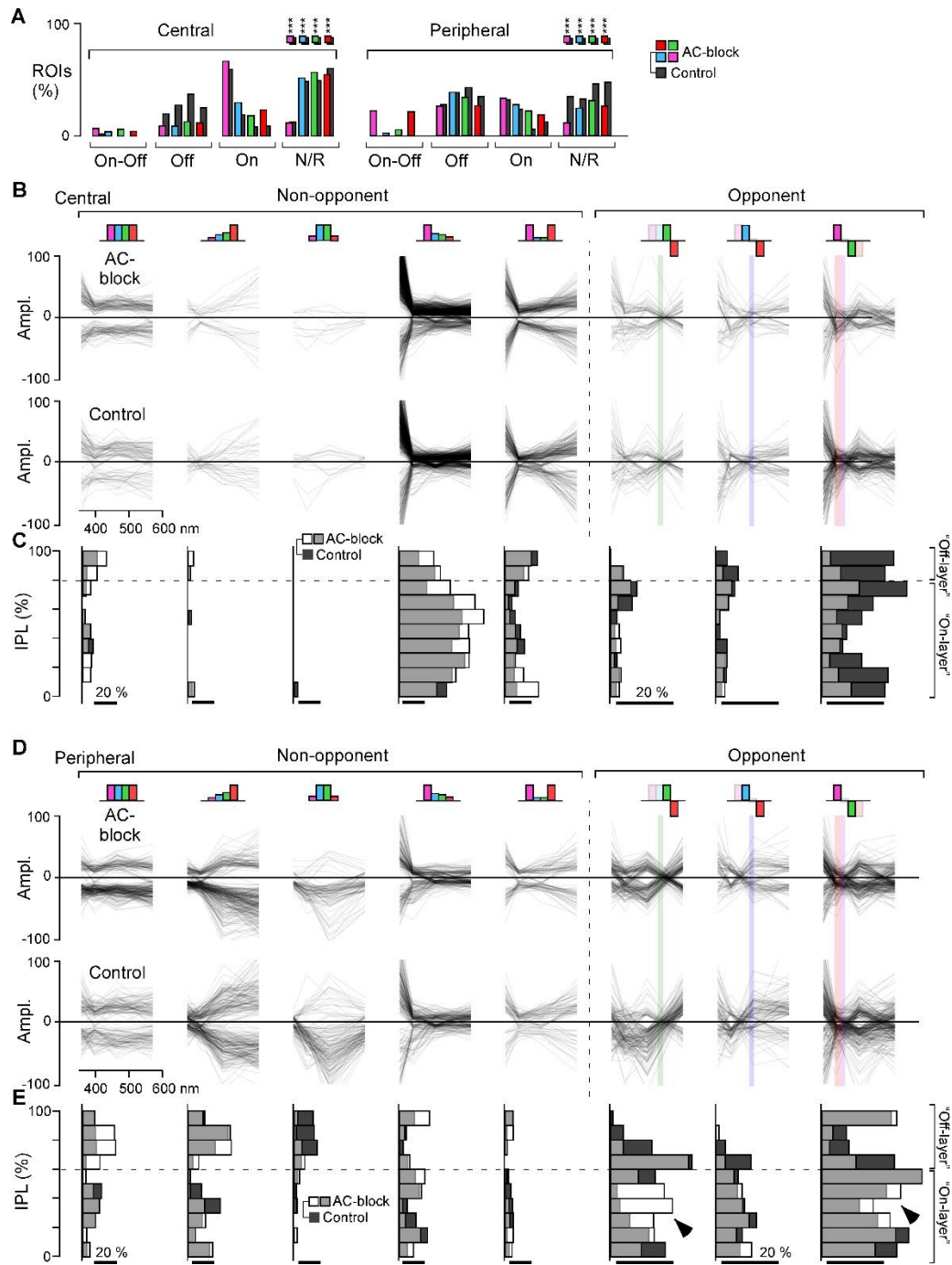
Supplemental Figure S4 – Result of alternative clustering, related to Figure 2. ROIs from the central and peripheral retina were clustered independently.



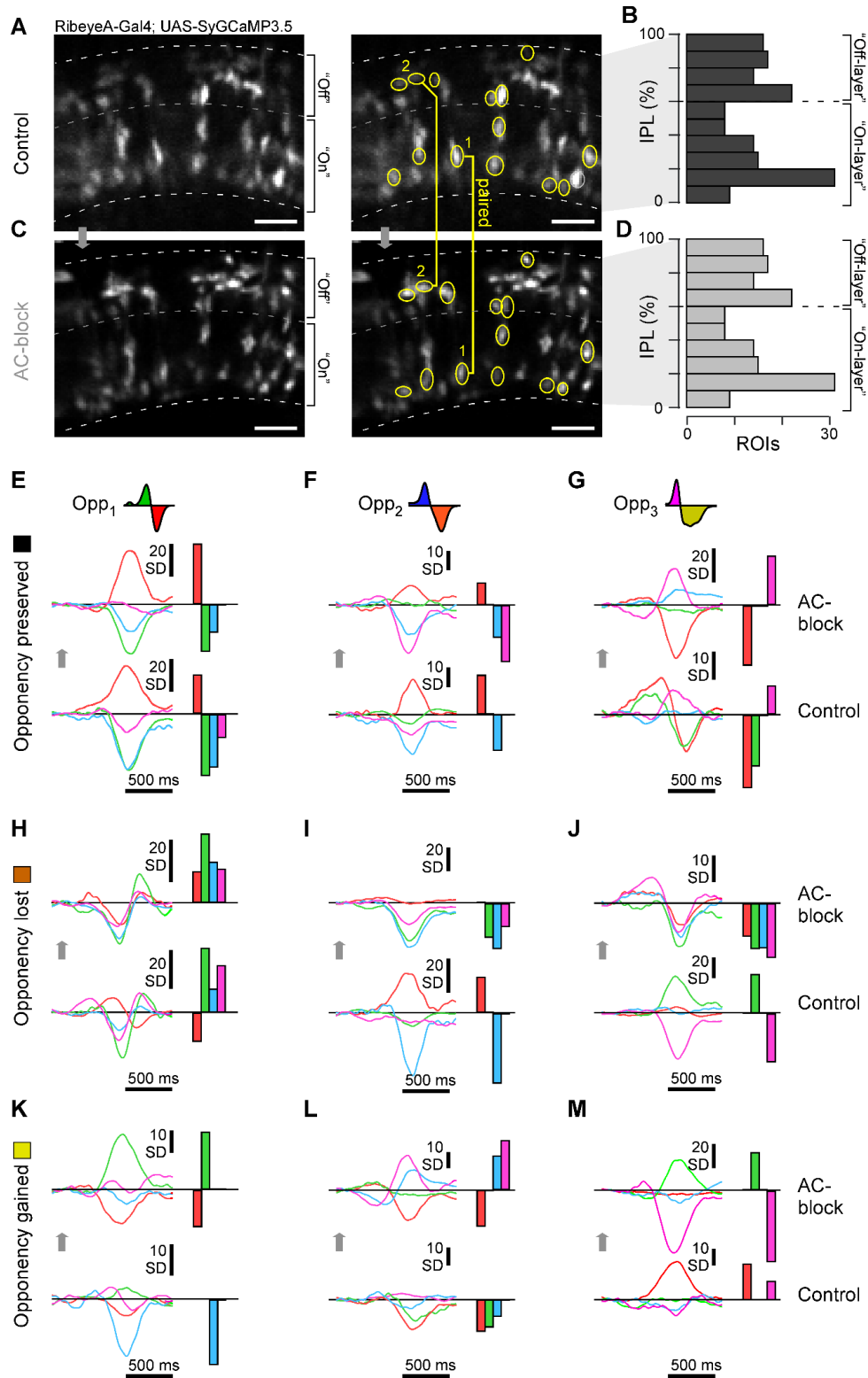
Supplemental Figure S5 – Cone fitting of the AC-clusters, related to Figure 3. **A**, Distribution of AC-clusters across the four spectral groups (cf. Figure 3A-D), divided by retinal location: Central (black), Peripheral (white) and mixed (grey). **B**, Spectral relationship of cone-photoreceptor outputs (thin lines, based on Ref⁷), their spectral zero crossings (shaded bars, labelled "opponencies"), and the spectra of the four LEDs used to probe ACs and BCs in the present study (solid curves). Note that the spectral zero crossings of blue-cones coincide with the bulk of the spectral power of the green-LED. **C**, Reduced spectral tuning functions of the cone outputs as they would appear if probed with the four LEDs used in the present study. Note that the specific LED placement resulted in an under sampling of the full blue-cone opponency. **D,E**, Cone-weights (D) and overview of fits (E) between spectral tuning functions of reduced cones (see above) and AC-cluster means. The four plots in (D) part-correspond to the four spectral groups shown in Figure 3A-D, however with On- and Off versions of long-wavelength biased clusters combined (D, top), while the five color-opponent clusters were further subdivided into two separate groups as shown (D, bottom). (E) shows one panel per cluster as indicated, sorted by spectral groups. Shown are: AC-cluster mean (grey, thick), the best fit when using all four cones (black) and the fit result when only using red- and UV-cones (red, dashed). We also show the fit results for the six opponent clusters (bottom row) when using only green- and UV-cones (green, dashed) and when using red-, green- and UV-cones (light blue, dashed). For quantitative evaluation of fits, see Methods.



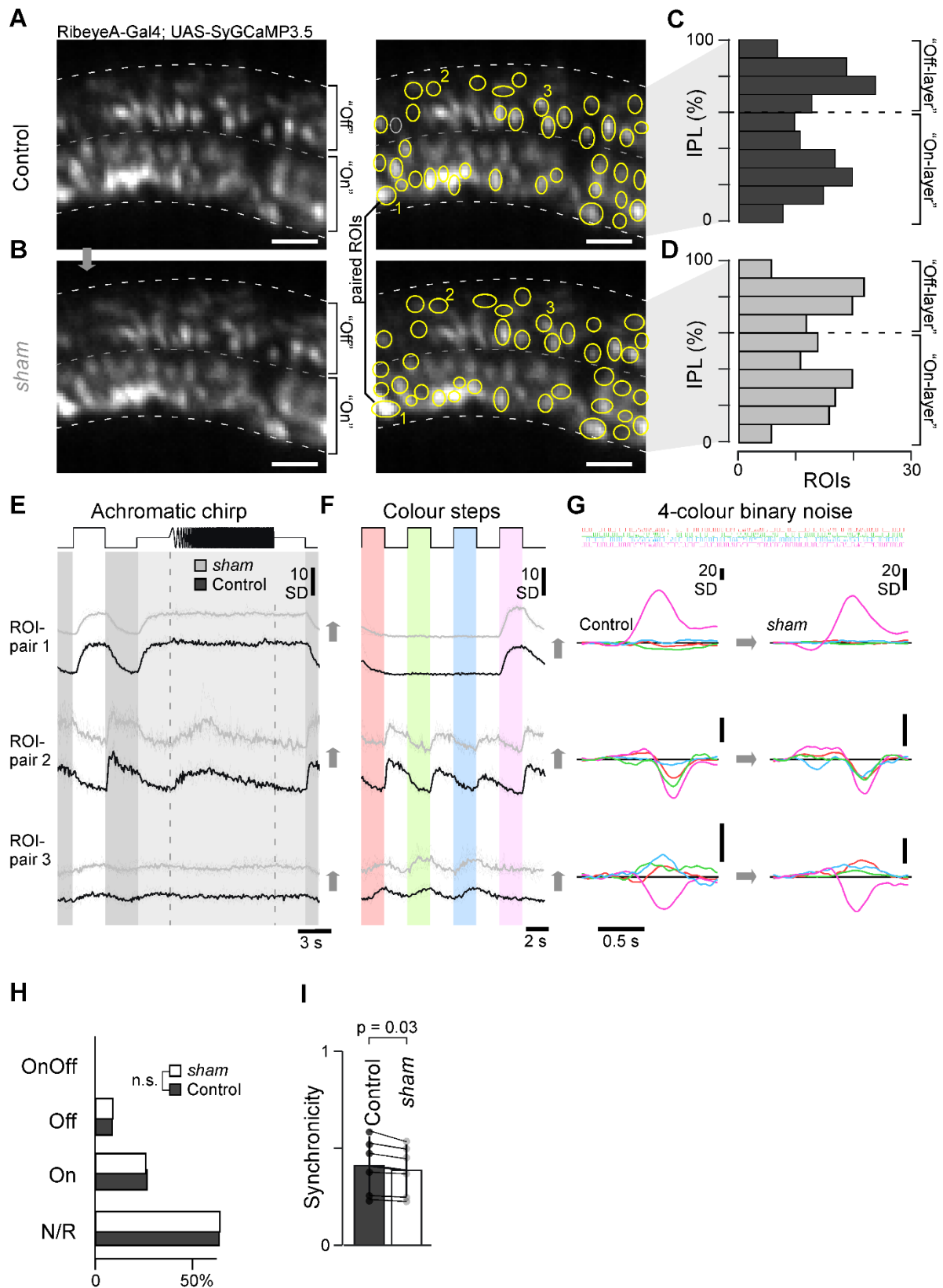
Supplemental Figure S6 – BC population synchronicity comparison and drug injection effect on four types of cones, related to Figure 4. **A,B**, comparison of population synchronicity during spectral noise stimulation. Heatmaps show the first 60 s of the z-normalised responses example scans during control conditions and following AC-block, as indicated, for the central retina (top two rows) and the peripheral retina (bottom two rows). Population synchronicity (**B**) was computed as in Ref⁶⁴. Wilcoxon Signed-Rank test: Central: $p < 0.001$; Peripheral: $p < 0.001$; Difference in change between central and peripheral: $p = 0.017$. **C-N**, No effect of drug-cocktail injection as in Figure 4 on spectral tuning including opponency in cones. Heatmaps (**C**) of SyGCaMP6f responses in red cone terminals to the four steps of light as Figure 4D based on previously established protocols⁷ before (bottom) and after drug injection (top), the same data summarised with mean ± 1SD shading (**D**) and extracted response amplitudes ± 1SD plotted against stimulus wavelength, with each curve's peak hyperpolarising response normalised to 1 (**E**). **F-N**, as (**C-E**), but for green (**F-H**), blue- (**I-K**) and UV-cones (**L-N**), respectively. The colored shadings in **H** and **K** indicates the spectral position of the green- and blue-cones' zero-crossings, respectively, from Ref⁷. Wilcoxon rank sum tests were used for comparing amplitude-normalized tuning functions, $p > 0.05$ for all the four types.



Supplemental Figure S7 – Distribution of BC-ROIs for color steps and spectral tuning function, related to Figure 5. **A**, As bar plot in Figure 5A,B, but here shown separately for the four color steps (cf. Figure 4D) instead of the single white step. Chi-squared tests were used to test for within-color changes in the distribution of terminals by polarity, $p < 0.001$ for all four colors. **B**, All central BCs' spectral tuning functions (based on the kernels, cf. Figure 4E) under control (bottom) and AC-block condition (top) sorted into nine categories as indicated (Methods, cf. Figure 5G,H, plotted in same order). Individual BCs are plotted as semi-transparent grey such that darker shades overall indicate larger numbers of BCs. The colored vertical bars in the three opponent groups (right) indicate their corresponding spectral zero crossings (based on Refs^{7,18} – cf. Supplemental Figure S5B,C). **C**, As Figure 5I,J, data from (A) summarised by IPL position. **D,E**, as (B,C), respectively, but for Peripheral retina. Arrowheads indicate IPL regions where the representation of spectral opponency systematically increases following AC-block. Two sample Kolmogorov–Smirnov tests, Central, $p > 0.05$; Peripheral, $p < 0.001$.

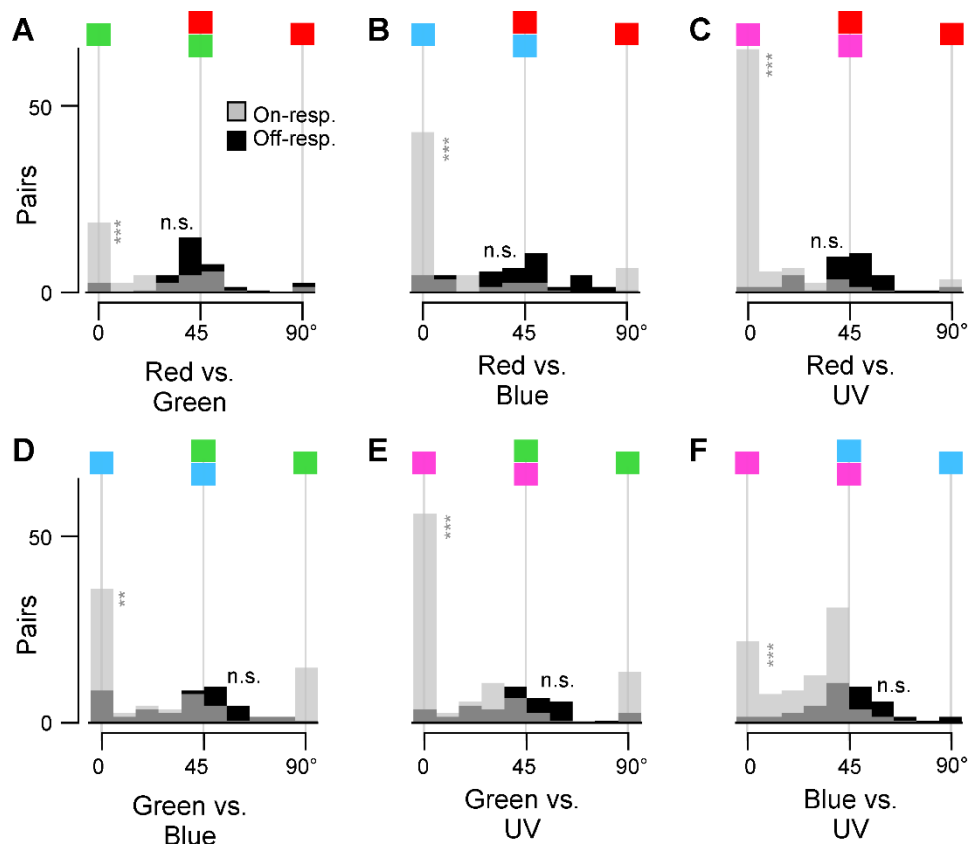


Supplemental Figure S8 – Example data of paired BC recordings with drug injection, related for Figure 6.
A-D, Example scan field with BCs sparsely expressing SyGCaMP3.5 under control conditions (**A**) and the same field of view following AC-block (**B**). Approximately half of visible BC terminals could be reliably matched across the two conditions (yellow) and were counted as paired data. Paired terminals spanned the entire depth of the IPL (**B,D**). **E-M**, Selected example BCs (paired data) that either preserved (**E-G**), lost (**H-J**) or gained (**K-M**) spectral opponency following pharmacological removal of inner retinal inhibition. Examples from all three types of opponencies are presented: red:green (Opp₁, **E,H,K**), red/(green):blue (Opp₂, **F,I,L**), (red)/green:UV (Opp₃, **G,J,M**). Shown in each case are the four spectral kernels (left) and their automatically extracted response amplitudes (right, Methods).



Supplemental Figure S9 – sham injection results, related for Figure 6

A-G. As [Supplemental Figure S8A-D](#) and [Figure 6A-C](#), respectively, but here shown for sham injection dataset. **H.** No change in response allocation based on the white step responses in the sham dataset before (dark grey) and after sham injection (white). Chi-squared test, $p > 0.05$. **I.** No change in population synchronicity in sham dataset. Wilcoxon Signed-Rank test: $p = 0.03$. (cf. [Supplemental Figure S6B](#)).



Supplemental Figure S10 –comparison of response amplitude changes across different pairs of wavelengths, related to Figure 7. A-F, as Figure 7F, but for all six possible color combinations. Wilcoxon Signed-Rank tests On: $p < 0.001$ for all the combinations; Off: $p > 0.05$ for all the combinations.